ACS Sustainable Chemistry & Engineering

Research Article

pubs.acs.org/journal/ascecg

Green Poly(ε-caprolactone) Composites Reinforced with Electrospun Polylactide/Poly(ε-caprolactone) Blend Fiber Mats

Jianxiang Chen,[†,‡] Liangliang Lu,[†,‡] Defeng Wu,*[,†,‡] Lijuan Yuan,[†,‡] Ming Zhang,[‡,§] Jingjing Hua,[†] and Jia Xu[†]

[†]School of Chemistry and Chemical Engineering, Yangzhou University, 180 Siwangting Road, Yangzhou, Jiangsu 225002, P. R. China

[‡]Provincial Key Laboratory of Environmental Material and Engineering, 180 Siwangting Road, Yangzhou, Jiangsu 225002, P. R. China

[§]Testing Center, Yangzhou University, 48 East Wenhui Road, Yangzhou, Jiangsu 225009, P. R. China

Supporting Information

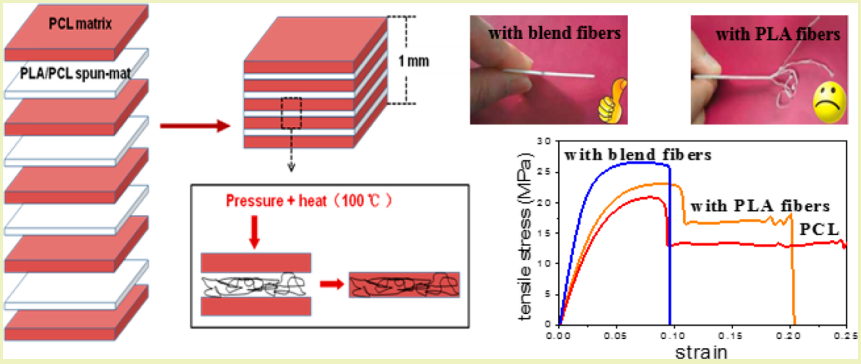

ABSTRACT: As two typical aliphatic polyesters, biodegradable poly(ε-caprolactone) (PCL) and polylactide (PLA) show quite different mechanical properties. Compounding them together is therefore an interesting topic on the fabrication of biomaterials with tailorable properties. The composite technology was used in this work to prepare a new PCL/PLA system, the green PCL composites reinforced with the electrospun PLA fibers. The minor PCL was then introduced into the PLA fibers to improve the reinforcing effect further. The results reveal that PLA can act as good reinforcement to PCL in the way of continuous fibers because the PCL composites reinforced with the PLA fiber mats show far higher strength and modulus than those of neat PCL and the PCL/PLA blend samples prepared by melt mixing. In comparison with the neat PLA fibers, the PLA/PCL blend fibers have a better reinforcing effect to PCL. The presence of a minor PCL component in the electrospun blend fibers improves the affinity between the fibers and PCL matrix by reducing fiber−matrix interfacial tension and enhances interfacial adhesion via mutual fusion between the fiber surface PCL phase and matrix PCL during hot compression. Both the mechanical properties and the viscoelastic responses of the composites are highly dependent on the fiber contents and PLA/PCL ratios of the blend fibers. The presence of superfluous fiber-contained PCL has no more contribution to affinity improvement and could even decrease the reinforcing effect because of degraded fiber strength. Thus, the PLA/PCL weight ratio of the blend fibers is vital to the final properties of the fiber-reinforced PCL green composites.

KEYWORDS: *Poly(ε-caprolactone), Polylactide, Electrospun blend fibers, Fiber reinforcements, Green composite*

INTRODUCTION

In the past several decades, environmental concerns and a shortage of petroleum resources have driven efforts to develop new bulk production of bio-originated and biodegradable polymers.[1] More and more biopolymers with environmentally friendly characteristics, such as aliphatic polyesters, unsaturated polyesters, polysaccharides, and modified polyolefins, have been developed to replace the traditional synthetic polymers.[2] To further extend the applications of those biopolymers, a convenient blending technology is commonly employed.[3] For instance, two typical biodegradable aliphatic polyesters, polylactide (PLA) and poly(ε-caprolactone) (PCL), show quite different mechanical properties and biodegradability.[4] The glassy PLA presents better tensile strength and a higher degradation rate, while the rubbery PCL presents better toughness and a much slower degradation rate. Therefore, blending them together is an efficient strategy to tailor the properties and lifetime according to different environmental or physiological requirements.[5−13]

However, the two biodegradable polymers, PLA and PCL, are immiscible thermodynamically, and the phase separation and poor interfacial adhesion highly restrict property

Received: January 17, 2014
Revised: July 8, 2014
Published: August 11, 2014

combinations of their blends. A common way of improving the phase morphology and final properties of the PLA/PCL blend system is to use the well-defined di-block or tri-block copolymers as the compatibilizer to emulsify phase interface and reduce interfacial tension.[14−17] The anisotropic nanoparticles such as carbon nanotubes (CNTs) can also be used as the third component to refine phase size of the PLA/PCL blends through controlling the interfacial location of CNTs because the selective localization of CNTs not only prevents coalescence of the discrete domains but also enhances the interfacial adhesion.[18−20] In this case, the CNTs act as the reinforcements and compatibilizer simultaneously, improving the final morphology and properties of the PLA/PCL blends.

Regardless of whichever approach mentioned above is used, the discrete phase in the blends commonly presents discontinuous domain morphology. That means that the phase interface area is limited. It is well known that the fiber reinforcement is a very efficient strategy to improve the mechanical properties of polymers because the larger interfacial area between fibers and matrix polymers, which is caused by the special aspect ratio structure of continuous fibers, favors strengthening the overall interfacial interactions.[21] Reducing fiber size from micron scale to nanoscale can further enhance interfacial adhesion because the special surface area of the fibers increases in this case by several orders of magnitude.[22] Electrospinning is a handy approach to produce fibers with diameters ranging from nanoscale to submicron scale,[23] which are typically one or two orders of magnitude lower than those of the fibers fabricated by routine solution spinning. Thus, it provides a new way to manufacture the reinforced polymer composites with polymer fibers instead of using traditional inorganic fibers such as glass fibers and carbon fibers.[24] Actually, this kind of polymeric composite reinforced with electrospun polymer fibers has already attracted some attention.[25−38] The concept was first proposed by Kim and Reneker.[25] They prepared the electrospun fiber-reinforced epoxy resin composites by impregnation of the electrospun fiber mats with a matrix polymer through compression molding. The as-obtained composites present far higher Young's modulus than that of the neat epoxy resin, even at the very lower electrospun fiber contents. A similar reinforcing effect of the electrospun nylon fibers were also observed on some other polymer systems.[26−30]

This new composite technology can also be applied on the PLA/PCL system because the two components, PLA and PCL, are asymmetric thermodynamically. PLA shows far higher glass transition temperature and melting point than PCL, which means that the PLA component could maintain its continuous fiber morphology over the processing temperature of PCL, if utilizing the electrospun PLA fibers as reinforcement to the PCL matrix. This is a new path to fabricate PLA/PCL material with high performance without addition of any third component, especially the nondegradable inorganic nanoparticles. In general, the system containing the biopolymer matrix and reinforcements or filler coming from natural or renewable or bio-originated mass is commonly referred to as "green".[39−42] Thus, the PLA fiber-reinforced PCL is a typical green composite. Furthermore, introducing a small amount of PCL into the electrospun PLA fibers is possible to improve affinity between the PCL matrix and PLA fibers. It was found in our previous work[43] that the phase separation between PCL and PLA existed from the inside to the surface of the electrospun PLA/PCL blend fibers. The discrete PCL phase showed an elongated morphology along with a fiber axis with a very fine diameter instead of the droplet structure. This suggests that as the fiber reinforcement, the PLA/PCL blend fiber may be better than the neat PLA fiber because the presence of the minor PCL phase in the blend fibers can reduce the interfacial energy between fibers and PCL matrix. On the other hand, mutual fusion between the fiber surface PCL and matrix PCL may further improve interfacial adhesion between fiber layers and PCL layers during hot compression if the compression temperature is higher than the melting point of PCL but lower than that of PLA. Therefore, the electrospun PLA and PLA/PCL blend fiber mats were used as the reinforcements in this work to prepare PCL composites. Then, the effects of the fiber PLA/PCL ratio and PLA mass contents on the mechanical properties and morphology of the composites were studied in detail, aiming at exploring a new way to combine complementary properties of PLA and PCL and finally obtain green PLA/PCL materials with a tailorable property. It is well known that PCL can be used for series applications, such as disposable food service items, food packaging, health care products, and agricultural films.[44] Using electrospun PLA or PLA/PCL blend fiber mats as the reinforcements, on the one hand, can control the degradation rate of the PCL-based end-products because PLA shows a far higher rate of degradation than PCL, and on the other hand, they can improve the mechanical strength of those end-products to better meet the requirements of food packaging and medical devices.

EXPERIMENTAL SECTION

Materials and Prepration. PLA (2002D) is a commercial product of Nature Works Co., Ltd. (U.S.A.). It has a *D* content of 4.25 wt %, a residual monomer content of 0.3 wt %, and a density of 1.24 g cm^{-3}, with a melt index (MI) of 8 g/10 min (190 °C/2.16 kg, ASTM D1238). Its number-average molecular weight (M_n) is about 100,000. PCL (CAPA6500) used in this work is also a commercial product purchased from Solvay Co., Ltd. (Belgium). It has a −OH value of lower than 2 mg KOH g^{-1}, with a MI of 7 g/10 min (160 °C/2.16 kg, ASTM D1238) and a M_n of 60,000. The differential scanning calorimetry (DSC) thermograms of these two polymers are shown in Figure S1 of the Supporting Information. The two solvents of chloroform (CF) and dimethylformamide (DMF) are all AR and purchased from Sinopharm Chemical Reagent. The polymers were dried before use, and all materials were used without further purification.

First, PCL sheet samples (10 cm × 10 cm) with a thickness of about 0.2 mm were prepared by compression molding at 100 °C and 15 MPa. Second, the sheet samples were placed on a grounded metal target of an electrospinning system to be coated with electrospun PLA or PLA/PCL blend fibers and then vacuum-dried at 30 °C for 48 h to remove residual solvents. The morphology of the neat and coated PCL sheets are shown in Figure S2 of the Supporting Information. Finally, those sheets were alternatively superposed (15−20 layers), followed by compression molding (120 °C and 15 MPa) to make the electrospun fiber mats impregnated with matrix PCL, as schematically illustrated in Figure 1. As for the electrospinning of PLA/PCL blend fibers, the detailed electrospinning procedures of blend fibers were reported in the previous work.[43] First, the PLA/PCL blends with different blending ratios were dissolved in a mixture of CF/DMF (w/w = 4/1) to form solutions with predetermined concentrations. Then, the solution was loaded in a syringe with a metal capillary attached for electrospinning. The parameters of electrospinning are given in Table S1 of the Supporting Information. Hereafter, the electrospun blend fiber mats are referred to PLA*x*/PCL*y*, where *x* and *y* are the weight ratios of PLA and PCL components per 100 weight of fiber mats, respectively. The obtained PCL composites are abbreviated to (PLA*x*/

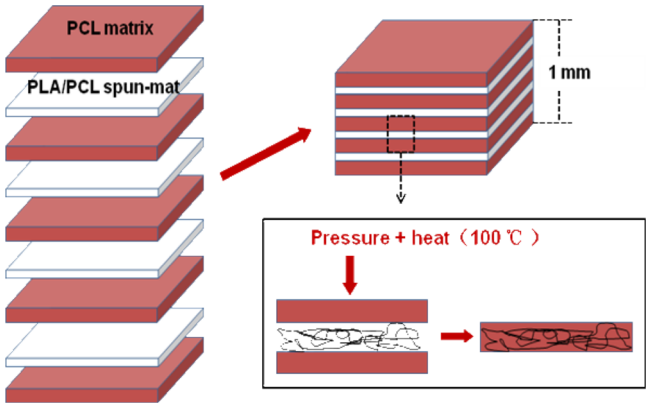

Figure 1. Schematic illustration of the fabrication of PCL composites with electrospun PLA/PCL blend fiber mats.

PCL*y*)C*z* (C means the composite, *z* is the weight ratio of PLA component per 100 weight of composite, and PLA*x*/PCL*y* is the composition (PLA/PCL w/w) of blend fibers). Here, using the PLA weight ratio rather than the fiber mass ratio to describe the composite compositions is more reasonable because surface PCL on the blend fiber mats was molten and finally fused with the matrix PCL during hot compression. In this case, the fiber mass ratio was altered and hence unsuitable to represent the composite compositions. A blend sample with the PCL/PLA weight ratio of 85/15 was prepared through melt mixing for the property comparison using the Haake Polylab Rheometer at 180 °C and 50 rpm, followed by compression molding at 180 °C and 15 MPa.

Contact Angle Measurements. Contact angle measurements were used here to evaluate the surface parameters of solid samples. The surface energy of a solid or a liquid consists of two components, the dispersive and polar components,[45]

$$\gamma_s = \gamma_s^d + \gamma_s^p \quad (1)$$

and the relations between contact angle and surface energy can be described by the Owens−Wendt method[46]

$$\gamma_l(1 + \cos\theta) = 2(\gamma_s^d\gamma_l^d)^{1/2} + 2(\gamma_s^p\gamma_l^p)^{1/2} \quad (2)$$

where γ_l and γ_s are the surface energy of the liquid and solid, respectively, and γ_s^d, γ_s^p, γ_l^d, and γ_l^p the dispersive and polar components of the solid and liquid, respectively, while θ is the contact angle. If the contact angles of at least two liquids, usually a polar and nonpolar liquid[47] with known γ_l^d and γ_l^p parameters, are measured on a solid surface, the γ_s^d and γ_s^p parameters as well as the surface energy γ_s of that solid can be calculated.

Contact angle tests were performed with an OCA40 apparatus (Dataphysics Co., Ltd., Germany). Static contact angles of two test liquids (distilled water and glycerol) were measured by depositing a drop of 3−5 μL on the sample surface, and the values were estimated as the tangent normal to the drop at the intersection between the sessile drop and the surface. To avoid solvent evaporation, images were taken within 30 s of drop deposition. The reported contact angle values here are the average of five tests at different spots of the surface. The surface parameters of the tested samples were then calculated, and the results are listed in Table 1. Here, the literature values of surface parameters for the test liquids (20 °C) were used.[48] The values of interfacial energy between two solids can then be calculated according to the harmonic-mean equation[49]

$$\gamma_{12} = \gamma_1 + \gamma_2 - 4\left[\frac{\gamma_1^d\gamma_2^d}{\gamma_1^d + \gamma_2^d} + \frac{\gamma_1^p\gamma_2^p}{\gamma_1^p + \gamma_2^p}\right] \quad (3)$$

The results are also listed in Table 1.

Morphology Observation. The morphology of electrospun fiber mats was observed by an optical microscope (LEICA BX51, Germany) equipped with a hot stage (Linkam LTM350, U.K.) and also explored by a scanning electron microscope (SEM) (XL-30ESEM, Philips Co., The Netherlands) with 20 kV accelerating voltage. The number-average diameter of blend fibers were determined according to the following relation

$$D_n = \frac{\sum_i n_i D_i}{\sum_i n_i} \quad (4)$$

where n_i is the number of fibers with diameter of D_i counted from SEM images. The total number of fibers is about 100 in the analysis. The fractured surface of the tensile samples and the brittle-fractured samples was observed by a S-4800 field-emission scanning electron microscope (FE-SEM) (Hitachi Co., Japan) with 15 kV accelerating voltage.

Table 1. Surface Parameters of Sheet Samples and Values of Interfacial Energy between Neat PCL and Fiber Mat Samples

	surface parameters (mN/m)[a]			interfacial energy (mN/m)[b]
sheet sample	γ_s^d	γ_s^p	γ_s	γ_{12}
PCL	6.81	31.11	37.92	/
PLA[c]	3.24	37.21	40.45	1.88
PLA90/PCL10[c]	5.52	32.84	38.36	0.86
PLA80/PCL20[c]	4.67	32.42	37.09	0.68
PLA70/PCL30[c]	5.12	33.64	38.76	0.65

[a] γ_s^d and γ_s^p are the dispersive and polar components of solid sheet samples, respectively. [b] γ_{12} is the interfacial energy between the PCL sheet samples and other four sheet samples; [c] These four blend fiber mat samples experienced hot compression at 100 °C and 15 MPa.

Mechanical Property Tests. The tensile properties of the composites were determined according to ASTM D638 using a universal testing machine (Instron Co., Ltd., U.S.A.) at a crosshead speed of 100 mm/min at room temperature. Property values reported here represent an average of the results for tests run on six specimens.

Rheological Measurements. Rheological tests were carried out on a rotational rheometer (HAAKE RS600, Thermo Electron, U.S.A.) equipped with a parallel plate geometry using 20 mm diameter plates. The sheet samples were molten for 3 min in the fixture to eliminate residual thermal histories and then experienced a dynamic frequency sweep under a small amplitude oscillatory shear (SAOS) flow at 100 °C, during which the modulus and viscosity responses were recorded. The strain level (1%) was predetermined by the dynamic strain sweep.

RESULTS AND DISCUSSION

Determination of Electrspun Fiber Mats Used as Reinforcement. The effect of electrospinning parameters on the blend fiber morphology has been explored in detail in previous work.[43] The results reveal that the fibers with lower PCL mass fraction show better morphology with larger average fiber diameter than those of the fibers with higher PCL mass fraction. A small addition of DMF as the assistant solvent favors further improvement of fiber morphology because of the synergistic effects by improved conductivity and altered viscosity of the electrospun solutions. Although the as-obtained blend fibers show a smooth surface structure, the phase separation between PCL and PLA occurs inside the fibers because the two components are thermodynamically immiscible. To be used as the fiber reinforcement, the electrospun PLA/PCL blend fibers should maintain their continuous fiber morphology. The low melting point PCL component in the blend fibers, however, will be molten during hot compression with the matrix PCL. This means that the minor PCL phase must be discrete in the blend fibers, and only in this case, can PLA fully contribute its higher strength and modulus to the

composites through its continuous fiber structure. Figure 2 gives the optical images of the electrospun fibers with various

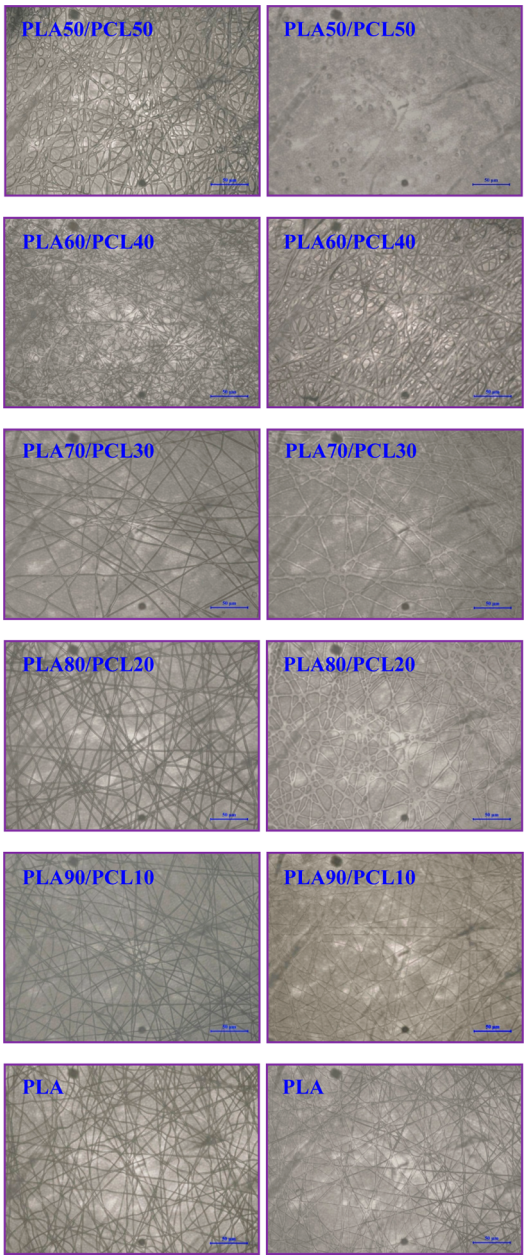

Figure 2. Optical images of electrospun PLA/PCL fibers at 120 °C (left) and 160 °C (right) with a scale bar of 50 μm.

PLA/PCL ratios at 120 and 160 °C (melting points of PLA and PCL are about 165 and 60 °C, respectively.). It is shown that the PLA50/PCL50 and PLA60/PCL40 fibers show a transparent appearance at 120 °C, and as the temperature achieves up to 160 °C, the fibers are coalesced with each other or even become discrete domains. This means that those two kinds of blend fibers cannot be used as the reinforcement because their continuous phase is PCL rather than PLA. As for the other three blend fiber mats, they are clearly in the solid state with an opaque appearance at 120 °C and can keep their continuous fiber morphology well at 160 °C, indicating that they may be suitable to be applied as the fiber reinforcement to PCL because PLA is the continuous phase in the fibers.

To explore the reinforcing effect of the blend fibers with various PLA/PCL ratios, it is necessary to avoid any possible interference caused by other aspects, such as fiber diameter. It is well known that the specific surface area of the electrospun fiber mats depends on the fiber diameter strongly.[50] Reducing the fiber diameter can increase the specific surface area of the fiber mats evidently because the electrospun fiber is of submicron scale or even nanoscale. As mentioned in the Introduction, the interfacial adhesion, which is closely related to the specific surface area of fibers,[22] is very important to a fiber-reinforced composite system. For better evaluation on the inter-relations between the reinforcing effect and PLA/PCL ratios of the blend fiber mats, therefore, it is necessary to reduce the diameter difference among those blend fiber mats to eliminate the influence of the fiber diameter on the interfacial adhesion as much as possible. At constant electrospinning conditions, the final morphology and size of the electrospun fibers are highly dependent on the electrospinning solution characteristics, such as solution viscosity, polarity, and solubility of solvent.[51,52] For the PLA/PCL blend fibers, the fiber diameter increases with an increase in solution concentrations at the constant blending ratio, while it decreases with increasing PCL content at the constant solution concentration because the presence of the PCL component reduces the solution viscosity.[43] Therefore, the fiber mats with different PLA/PCL ratios used in this work were obtained from the solutions with different concentrations (Table S2, Supporting Information). All blend fibers show very close values (~650 nm) of the average diameter.

Mechanical Properties of PCL Composites Reinforced by PLA/PCL Blend Fibers with Various PLA/PCL Weight Ratios. Figure 3 gives stress–strain curves of neat PCL, the

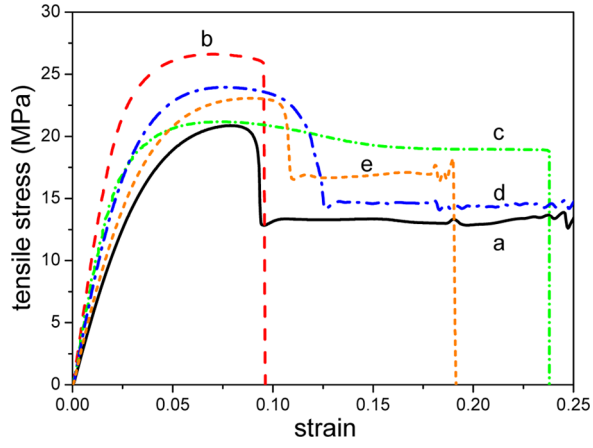

Figure 3. Tensile stress–strain curves of (a) neat PCL, (b) (PLA90/PCL10)C15, (c) (PLA80/PCL20)C15, (d) (PLA70/PCL30)C15, and (e) (PLA)C15 composite samples.

PLA/PCL blend prepared by melt blending, and the fiber-reinforced composite samples during tensile measurement. The obtained values of mechanical properties are listed in Table 2. Compared with neat PCL, the strength and modulus of the melt-mixed PLA/PCL blend sample decrease, indicating that simple blending is not an efficient way of combining the properties of PCL and PLA. This is attributed to macrophase separation with large domain size and as-resulted poor interfacial adhesion.[4,17,18] However, the composite with the neat PLA fiber mats has far higher values of strength and

Table 2. Tensile Properties of Neat PCL, PCL/PLA blend, and Composite Samples Containing Blend Fibers with Various PLA/PCL Ratios

sample	Young's modulus (MPa)	tensile strength (MPa)	elongation at break (%)
neat PCL	597.1 ± 26.3	20.9 ± 1.1	225.4 ± 50.0
PCL/PLA blend[a]	442.0 ± 29.1	20.6 ± 1.4	18.6 ± 3.6
PCL/PLA blend[b]	875.5 ± 28.9	22.3 ± 0.5	31.8 ± 5.6
(PLA)C15	692.7 ± 19.3	23.1 ± 0.4	20.1 ± 1.0
(PLA70/PCL30)C15	848.9 ± 30.9	23.1 ± 0.8	25.2 ± 2.2
(PLA80/PCL20)C15	964.0 ± 48.2	21.5 ± 1.7	23.7 ± 1.9
(PLA90/PCL10)C15	1144.5 ± 31.3	26.6 ± 1.5	9.5 ± 1.7
(PLA90/PCL10)C10	1036.4 ± 42.7	25.0 ± 0.2	5.0 ± 1.1
(PLA90/PCL10)C5	618.2 ± 73.0	25.1 ± 0.7	19.3 ± 3.1

[a]This sample was prepared by melt mixing with the PCL/PLA weight ratio of 85/15. [b]This sample was prepared by melt mixing with the PLA/PCL weight ratio of 70/30 using PLA-*b*-PCL di-block copolymers (M_n = 60 × 10^3 Dalton, composition$_{PCL:PLA}$ = 74:26, M_w/M_n = 1.75, 2 phr) as the compatibilizer. The mechanical property values here are reported in ref 17.

modulus than those of neat PCL, indicating that PLA can act as good reinforcement in the way of continuous fibers or fiber mats. It is notable that the strength of the composite with neat PLA fiber mats is even higher than the melt-mixed PLA/PCL blend using di-block PLA-*b*-PCL copolymers as the compatibilizer (detailed information on molecular characteristics of the used copolymers and on the mechanical testing results can be found in ref 17). This confirms that using electrospun fibers as the reinforcements may be a promising way of fabricating PLA/PCL biomaterials with high properties.

It is as expected that the blend fiber mats have a better reinforcing effect than the neat PLA fiber mats. In comparison with those of the (PLA)C15 sample, the modulus and strength values of the (PLA90/PCL10)C15 sample increase by about 65% and 15%, respectively. Although the modulus of the (PLA90/PCL10)C*s* samples decreases with increasing content of the low-modulus PCL component in the blend fiber mats, it is higher than that of the (PLA)C15 sample. This suggests that the presence of the PCL phase in the electrospun blend fiber mats could improve interfacial adhesion between the matrix PCL and fiber layers, which is confirmed by the SEM observation. Figure 4 shows the SEM images of the brittle-fractured surface of the composite samples reinforced by neat PLA and blend fiber mats. The layer-by-layer structure of the sample is shown in the inset graph. It is clear that the blend fibers are well embedded by the matrix PCL after hot compression, while the neat PLA fibers not fully wetted, showing a poor situation of interfacial adhesion. The presence of incompact interfacial layers or cavities has a negative contribution to the bulk modulus because of their far lower densities.[53,54] As a result, the role of fiber reinforcement is not fully played by the neat PLA fibers and is not up to the level by the blend fibers containing 30 wt % rubbery PCL, although the modulus of PLA fibers is far higher than the blend fibers. This elucidates the importance of affinity between the fiber mats and polymer matrix.

To further explore how the fiber-contained PCL improves affinity of the fiber mats to the matrix, the contact angle was measured for the surface property evaluation, as shown in Figure 5. Neat PLA and the blend fiber mats have the water and glycerol contact angles both far larger than 90°, showing typical hydrophobic and oleophobic surface characteristics. This interesting phenomenon has been widely observed on the

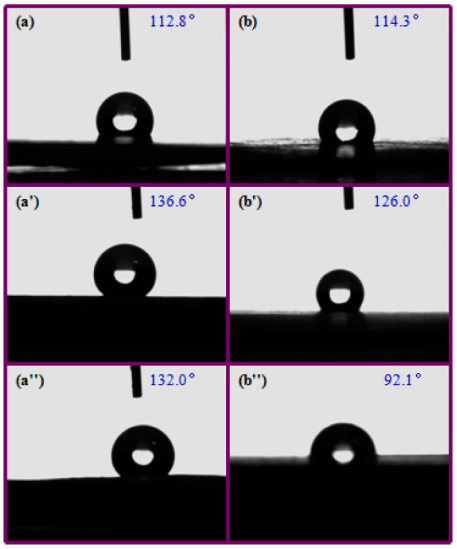

Figure 5. Contact angle images of (a,a″) PLA fiber mats and (b,b″) PLA70/PCL30 fiber mats measured at room temperature (Top: deionized water mats. Middle and bottom: glycerol mats). Samples shown in (a″) and (b″) were annealed at 100 °C for 10 min and then cooled to room temperature.

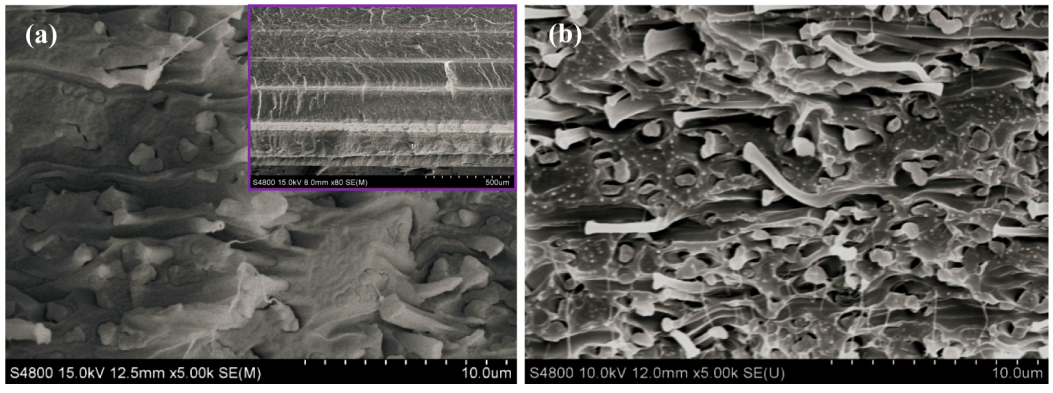

Figure 4. SEM images of brittle-fractured surface of (a) (PLA90/PCL10)C15 and (b) (PLA)C15 composite samples with a scale bar of 10 μm. The scale bar of inset graph is 500 μm.

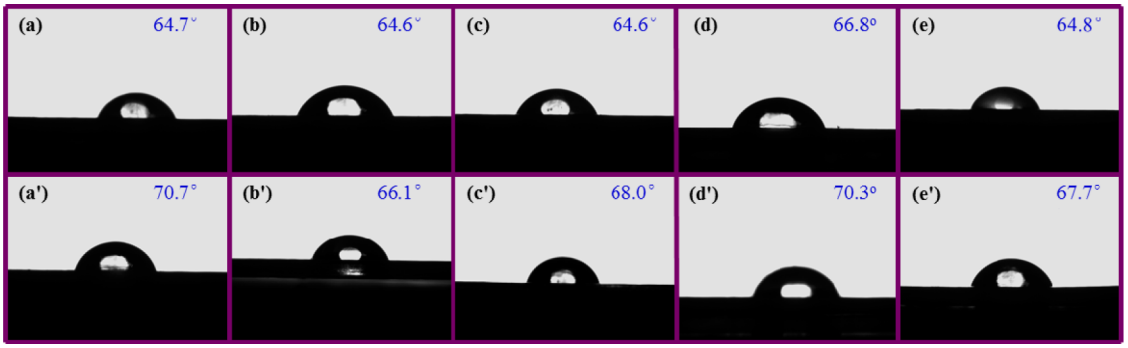

Figure 6. Contact angle images of (a,a′) PCL, (b,b′) PLA, (c,c′) PLA70/PCL30, (d,d′) PLA80/PCL20, and (e,e′) PLA90/PCL10 sheet samples (prepared by compression at 120 °C and 15 MPa using electrospun fiber mats except PCL sample) measured at room temperature (Top: deionized water, Bottom: glycerol).

electrospun membrane/array systems.[55−59] As is well known, the disordered packing of the nanofibers during electrospinning results in the formation of a rough surface and porous structure of the fiber mats. Accordingly, air is readily trapped in the surface pores or fiber gaps. In this case, the droplets stayed on the composite surface of the trapped air and solid, rather than in continuous contact with the solid surface.[55] The sharply increased contact area can increase the contact angle,[60,61] and as a result, the electrospun fiber mats commonly present a self-cleaning effect, similar to a lotus leaf.[56−58] Such kinds of hydrophobic or oleophobic surface characteristics, however, are highly dependent on the porous structure of the electrospun fiber mats. It is observed that the contact angle of the blend fiber mats decreases remarkably after being annealed at 100 °C (Figure 5 (b″)). This is because the molten surface PCL of the fibers spreads into the fiber gaps or pores and excludes the trapped air to some extent, reducing the surface area of the fiber mats finally. As for the neat PLA fiber mats, the annealing history nearly does not change their surface properties (Figure 5 (a″)) because the melting point of PLA is far higher than the annealing temperature.

However, the fiber-reinforced PCL composites were prepared by hot compression. That means that the surface PCL phase of the blend fibers is molten, and the porous structure of the mats may be highly squeezed under high temperature and pressure. Therefore, the hydrophobic or oleophobic surface parameters of the blend fiber mats obtained under room temperature and normal atmosphere are unsuitable to be used for evaluation of the interfacial property between PCL and fiber mats. Figure 6 shows the contact angle images of the samples that experienced hot compression (except the PCL bulk sheet). The obtained surface parameters and calculated values of interfacial energy are listed in Table 1. It is clear that the interfacial energy between the blend fiber mats and PCL is reduced by 1 order of magnitude relative to the neat PLA mats. This confirms that the affinity of the fiber mats to the matrix is improved effectively through introducing a matrix polymer phase into the electrospun fiber mats. It is notable that the hot-compressed blend fiber mat samples have interfacial energy values on the same order. This indicates that the presence of a small amount of PCL is enough to improve the affinity between the fiber mats and matrix PCL. In other words, an excessive PCL component in the blend fibers not only has no evident contribution to the affinity improvement between the mat layer and PCL layer but also reduces the fiber modulus and degrades the reinforcing effect. This is confirmed by the mechanical property tests shown in Figure 3.

The presence of PCL phase in the fiber mats can enhance interfacial adhesion through other approaches. It had been reported in our previous work[43] that the discrete PCL domain in the fibers showed an elongated morphology along the fiber axis during electrospinning. Thus, the rugged ravine-like structure forms on the fiber surface after the surface−PCL phase of the fibers is molten following hot compression, increasing the surface roughness as a result. On the other hand, those subsequently exposed PCL domains inside the blend fibers can be fused with the matrix PCL, further strengthening interfacial adhesion. Therefore, the sample reinforced with the blend fiber mats keeps its specimen morphology well after tensile tests, while the one with the neat PLA fiber mats is delaminated, as shown in Figure 7. This confirms the poor interfacial adhesion between the matrix layers and PLA fiber layers because the load transfer between the two layers is uneven, leading to interfacial delamination.

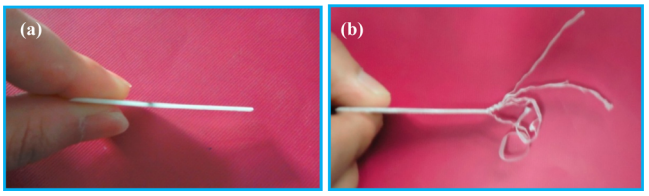

Figure 7. Optical images of side profile of (a) (PLA90/PCL10)C15 and (b) (PLA)C15 samples after tensile tests.

Effect of Fiber Contents on Mechanical and Rheological Properties of Reinforced Composites. The results above reveal that the blend fiber mats have a better reinforcing effect for the PCL than the neat PLA fiber mats. However, the presence of superfluous fiber-contained PCL degrades the reinforcing effect of the blend fiber mats. The PLA/PCL ratio of 90/10 is the best option for the blend fibers. The tensile curves of the composites with various PLA90/PCL10 fiber contents are shown in Figure 8, and the parameter values are listed in Table 2. Clearly, all composite samples show higher values of strength and modulus than those of the (PLA)C15 sample, even for the (PLA90/PCL10)C5 sample containing far lower fiber content. As discussed in the Experimental Section, the PLA mass ratio in the composite is used here to represent fiber content. With an increasing PLA mass ratio, the values of the modulus increase sharply, accompanied by little change of strength in the current ratio range. It is hard to further increase the mass ratio of PLA because the PCL mass also increases with

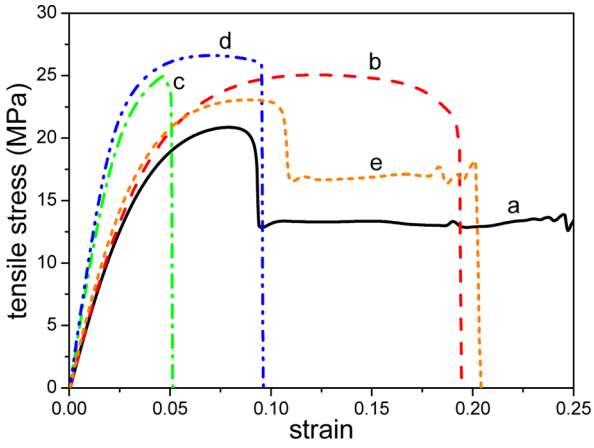

Figure 8. Tensile stress–strain curves of (a) neat PCL sample, (b) (PLA90/PCL10)C5, (c) (PLA90/PCL10)C10, (d) (PLA90/PCL10)-C15, and (e) (PLA)C15 composites.

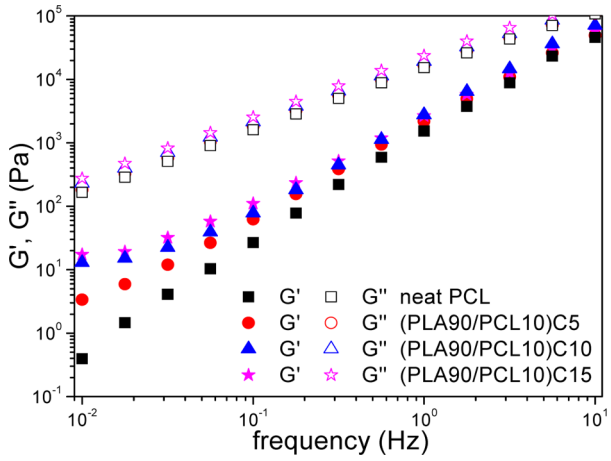

Figure 10. Dynamic storage modulus (G') and loss modulus (G'') versus frequency for the neat PCL and (PLA90/PCL10)C*s* samples (100 °C).

increasing blend fiber content. The SEM images of the broken surface of the tensiled samples are shown in Figure 9. Clearly, the break and pull-out of fibers are the main approaches of the dissipation of energy. However, only a few fibers are broken (arrows) or pulled out (circles) perpendicular to the fractured surface, and most of fibers are still well embedded by the matrix PCL, perpendicular to the elongation direction. This means that many fibers are not put into full play during load transfer.[53] But this also indicates that there is space to further improve reinforcement by the electrospun fibers.

The presence of fiber mats also has a visible influence on the viscoelastic behavior of PCL. Figure 10 presents the dynamic modulus of the neat PCL sample and its composites with various PLA90/PCL10 fiber contents. At the experimental temperature (100 °C), PLA is in its solid state with continuous fiber morphology. Thus, the shape relaxation shoulder cannot be observed on the modulus curves at the medium frequency because the composite is a fiber suspension system rather than a two-phase emulsion system.[61,62] Moreover, all composite samples show the values of the loss modulus (G'') higher than the storage modulus (G'), indicating that the viscoelastic responses of the composite system are still dominated by the viscous matrix in the presence of the fiber mats. This is reasonable because the fiber mats and matrix PCL are compounded layer by layer alternatively, forming a multi-layered structure in the composites. The fiber layers are fully separated, rather than interpenetrated with one another, as shown in the inset graph in Figure 4. In this case, the viscous flow is dominant during oscillatory shear instead of elastic deformation. However, the presence of fiber mats still has a contribution to the elasticity of the system. It is clear that the low-frequency storage modulus increases with increasing fiber content. During oscillatory shear flow, the total area of the interface and the interfacial energy are changing periodically,[63] and the corresponding relaxation time is much longer than that of the matrix polymer chain because the matrix–fiber interface is semi-regid.[64,65] The increase in total interfacial area, therefore, leads to an evident increase in the low-frequency storage modulus with increasing fiber content. Clearly, the alteration of the low-frequency modulus can be used as a probe to obtain information on the interface in a multi-phase system. Figure 11 gives the dynamic modulus of the two samples reinforced with the neat PLA and blend fiber mats, respectively. It can be concluded that the (PLA90/PCL10)C15 sample has a more total interfacial area or stronger fiber–matrix interface interactions[66] than the (PLA)C15 sample because the former shows the storage modulus with a higher value than the latter at the low-frequency region. This again confirms that the blend fiber mats have better affinity to the PCL than the neat PLA fiber mats.

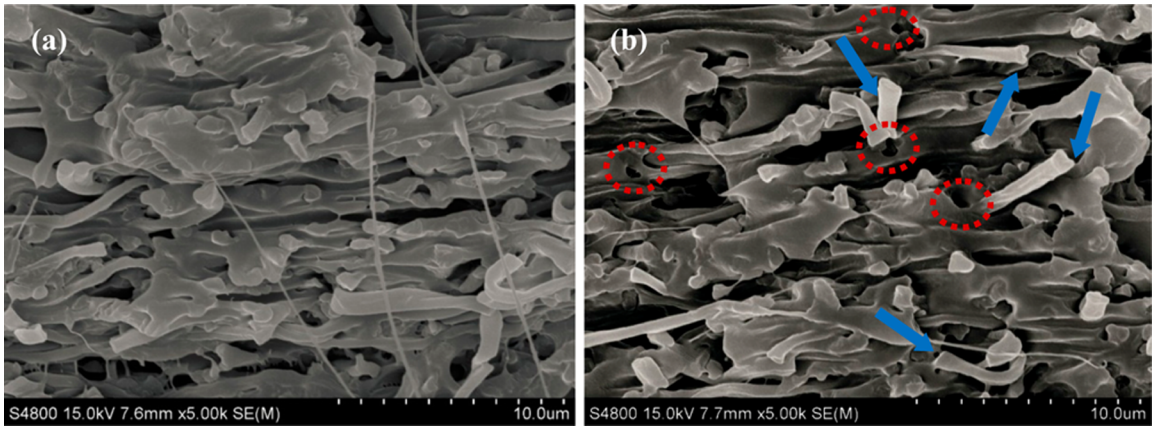

Figure 9. SEM images of broken surface of tensiled (a) (PLA90/PCL10)C10 and (b) (PLA90/PCL10)C15 samples with a scale bar of 10 μm.

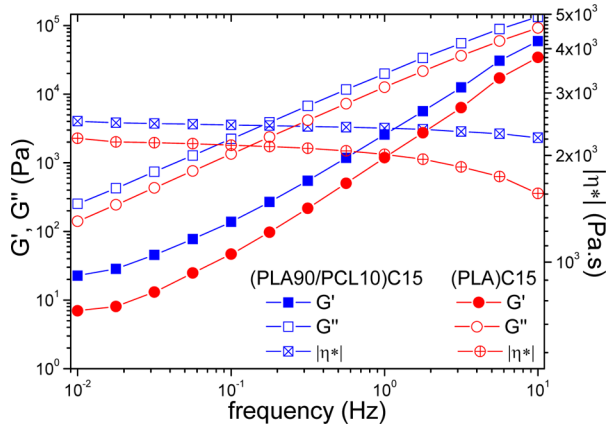

Figure 11. Dynamic storage modulus (G') and loss modulus (G'') as well as complex viscosity ($|\eta^*|$) versus frequency for the (PLA90/PCL10)C15 and (PLA)C15 samples (90 °C).

CONCLUSIONS

Electrospun PLA and PLA/PCL blend fiber mats can be used as the reinforcement to fabricate PCL-based green composites. The composite reinforced with the neat PLA fiber mats has lower modulus than those with the blend fiber mats. This is because the introduced minor PCL phase in the fibers improves the fiber−matrix affinity and enhances interfacial adhesion between the fiber mats and matrix layers. The mechanical properties of those composites depend strongly on the fiber contents and PLA/PCL ratios of the blend fibers. In the experimental content ranges, the strength increases with increasing fiber content. However, with an increase in the PCL ratio of the blend fibers, both the strength and modulus decrease because the excessive fiber-contained PCL phase degrades the strength of the blend fiber mats. Thus, the blend fiber with the PLA/PCL ratio of 90/10 is the best option to be used as the fiber reinforcement to prepare PCL/PLA biomaterials with high performance in this work.

ASSOCIATED CONTENT

Supporting Information

DSC scans, optical images, and tabulated data related to the electrospinning parameters and fiber diameters. This material is available free of charge via the Internet at http://pubs.acs.org.

AUTHOR INFORMATION

Corresponding Author

*Tel: +86-514-87975230. Fax: +86-514-87975244. E-mail: dfwu@yzu.edu.cn.

Notes

The authors declare no competing financial interest.

ACKNOWLEDGMENTS

This work was supported by research grants from the National Natural Science Foundation of China (51173156) and Qinglan Project of Jiangsu Province.

REFERENCES

(1) Vert, M.; Feijen, J.; Albertsson, A. C.; Scott, G.; Chiellini, E. *Biodegradable Polymer and Plastics*; Royal Society of Chemistry, London, 1992.

(2) Smith, R. *Biodegradable Polymers for Industrial Applications*; CRC Press: Boca Raton, FL, 2005.

(3) Eastmond, G. C. Poly(ε-caprolactone) blends. *Adv. Polym. Sci.* **2000**, *149*, 59−223.

(4) Wu, D. F.; Zhang, Y. S.; Zhang, M.; Zhou, W. D. Phase behavior and its viscoelastic responses of polylactide/poly(ε-caprolactone) blend. *Eur. Polym. J.* **2008**, *44*, 2171−2183.

(5) Gan, Z.; Yu, D.; Zhong, Z.; Liang, Q.; Jing, X. Enzymatric degradation of poly(ε-caprolactone)/poly(*D*, *L*-lactide) blends in phosphate buffer solution. *Polymer* **1999**, *40*, 2859−2862.

(6) Liu, L.; Li, S.; Garreau, H.; Vert, M. Selective enzymatic degradations of poly(*L*-lactide) and poly(ε-caprolactone) blend films. *Biomacromolecules* **2000**, *1*, 350−1359.

(7) Tsuji, H.; Ishizaka, T. Preparation of porous poly(ε-caprolactone) films from blends by selective enzymatic removal of poly(*L*-lactide). *Macromol. Biosci.* **2001**, *1*, 59−65.

(8) Dell Erba, R.; Groeninckx, G.; Maglio, G.; Malinconico, M.; Migliozzi, A. Immiscible polymer blends of semicrystalline biocompatible components: thermal properties and phase morphology analysis of PLLA/PCL blends. *Polymer* **2001**, *42*, 7831−7840.

(9) Broz, M. E.; VanderHart, D. L.; Washburn, N. R. Structural and mechanical properties of poly(*D*,*L*-lactic acid)/poly(ε-caprolactone) blends. *Biomaterials* **2003**, *24*, 4181−4190.

(10) Sarazin, P.; Roy, X.; Favis, B. D. Controlled preparation and properties of porous poly(*L*-lactide) obtained from a co-continuous blend of two biodegradable polymers. *Biomaterials* **2004**, *25*, 5965−5978.

(11) Roy, X.; Sarazin, P.; Favis, B. D. Ultraporous nanosheath materials by layer-by-layer deposition onto co-continuous polymer-blend templates. *Adv. Mater.* **2006**, *18*, 1015−1019.

(12) Sarazin, P.; Li, G.; Orts, W. J.; Favis, B. D. Binary and ternary blends of polylactide, polycaprolactone and thermoplastic starch. *Polymer* **2008**, *49*, 599−609.

(13) Zhang, Y. S.; Wu, D. F.; Zhang, M.; Zhou, W. D.; Xu, C. C. Effect of steady shear on the morphological evolution of biodegradable polylactide/poly(ε-caprolactone) blend. *Polym. Eng. Sci.* **2009**, *49*, 2293−2300.

(14) Maglio, G.; Migliozzi, A.; Palumbo, R.; Immirzi, B.; Volpe, M. G. Compatibilized poly(ε-caprolactone)/poly(*L*-lactide) blends for biomedical uses. *Macromol. Rapid Commun.* **1999**, *20*, 236−8.

(15) Na, Y. H.; He, Y.; Shuai, X. T.; Kikkawa, Y.; Doi, Y.; Inoue, Y. Compatibilization effect of poly(ε-caprolactone)-*b*-poly(ethylene glycol) block copolymers and phase morphology analysis in immiscible poly(lactide)/poly(ε-caprolactone) blends. *Biomacromolecules* **2002**, *3*, 1179−86.

(16) Li, S. M.; Liu, L. J.; Garreau, H.; Vert, M. Lipase-catalyzed biodegradation of poly(ε-caprolactone) blended with various polylactide-based polymers. *Biomacromolecules* **2003**, *4*, 372−7.

(17) Wu, D. F.; Zhang, Y. S.; Yuan, L. J.; Zhang, M.; Zhou, W. D. Viscoelastic interfacial properties of compatibilized polylactide/poly(ε-caprolactone) blend. *J. Polym. Sci., Part B: Polym. Phys.* **2010**, *48*, 756−65.

(18) Wu, D. F.; Zhang, Y. S.; Zhang, M.; Yu, W. Selective localization of multi-walled carbon nanotube in polylactide/poly(ε-caprolactone) blend. *Biomacromolecules* **2009**, *10*, 417−24.

(19) Laredo, E.; Grimau, M.; Bello, A.; Wu, D. F.; Zhang, Y. S.; Lin, D. P. AC Conductivity of selectively located carbon nanotubes in poly(ε-caprolactone)/polylactide blend nanocomposites. *Biomacromolecules* **2010**, *11*, 1339−47.

(20) Wu, D. F.; Lin, D. P.; Zhang, J.; Zhou, W. D.; Zhang, M.; Zhang, Y. S.; Wang, D. M.; Lin, B. L. Selective localization of nanofillers: effect on morphology and crystallization of PLA/PCL blends. *Macromol. Chem. Phys.* **2011**, *212*, 613−626.

(21) Pukanszky, B. Influence of interface interaction on the ultimate tensile properties of polymer composites. *Composites* **1990**, *21*, 255−262.

(22) Al-Saleh, M. H.; Sundararaj, U. A review of vapor grown carbon nanofiber/polymer conductive composites. *Carbon* **2009**, *47*, 2−22.

(23) Reneker, D. H.; Chun, I. Nanometre diameter fibres of polymer produced by electrospinning. *Nanotechnology* **1996**, *7*, 216−223.

(24) Huang, Z. M.; Zhang, Y. Z.; Kotakic, M.; Ramakrishna, S. A review on polymer nanofibers by electrospinning and their applications in nanocomposites. *Compos. Sci. Technol.* **2003**, *63*, 2223−2253.
(25) Kim, J. S.; Reneker, D. H. Mechanical properties of composites using ultrafine electrospun fibers. *Polym. Compos.* **1999**, *20*, 124−131.
(26) Bergshoef, M. M.; Vancso, G. J. Transparent nanocomposites with ultrathin electrospun nylon 4,6 fiber reinforcement. *Adv. Mater.* **1999**, *11*, 1362−1365.
(27) Fong, H. Electrospun nylon 6 nanofiber reinforced BIS-GMA/TEGDMA dental restorative composite resins. *Polymer* **2004**, *45*, 2427−2432.
(28) Neppalli, R.; Marega, C.; Marigo, A.; Bajgai, M. P.; Kim, H. Y.; Causin, V. Poly(ε-caprolactone) filled with electrospun nylon fibers: A model for a facile composite fabrication. *Eur. Polym. J.* **2010**, *46*, 968−976.
(29) Romo-Uribe, A.; Arizmendi, L.; Romero-Guzman, M. E.; Sepulveda-Guzman, S.; Cruz-Silvan, R. Electrospun nylon nanofibers as effective reinforcement to polyaniline membranes. *ACS Appl. Mater. Interfaces* **2009**, *1*, 2502−2508.
(30) Jiang, S. H.; Hou, H. Q.; Greiner, A.; Agarwal, S. Tough and transparent nylon-6 electrospun nanofiber reinforced melamine-formaldehyde composites. *ACS Appl. Mater. Interfaces* **2012**, *4*, 2597−2603.
(31) Liu, L.; Huang, Z. M.; He, C. L.; Han, X. J. Mechanical performance of laminated composites incorporated with nanofibrous membranes. *Mater. Sci. Eng., A* **2006**, *435*, 309−317.
(32) Liu, L.; Huang, Z. M.; Xu, G. Y.; Liang, Y. M.; Dong, G. H. Mode II interlaminar delamination of composite laminates incorporating with polymer ultrathin fibers. *Polym. Compos.* **2008**, *29*, 285−292.
(33) Li, G.; Li, P.; Yu, Y. H.; Jia, X. L.; Zhang, S.; Yang, X. P.; Ryu, S. Novel carbon fiber/epoxy composite toughened by electrospun polysulfone nanofibers. *Mater. Lett.* **2008**, *62*, 511−514.
(34) Han, S. O.; Son, W. K.; Youk, J. H.; Park, W. H. Electrospinning of ultrafine cellulose fibers and fabrication of poly(butylene succinate) biocomposites reinforced by them. *J. Appl. Polym. Sci.* **2008**, *107*, 1954−1959.
(35) Chen, G. F. S.; Liu, H. Q. Electrospun cellulose nanofiber reinforced soybean protein isolate composite film. *J. Appl. Polym. Sci.* **2008**, *110*, 641−646.
(36) Zhang, J.; Lin, T.; Wang, X. Electrospun nanofiber toughened carbon/epoxy composites: effects of polyetherketone cardo (PEK-C) nanofiber diameter and interlayer thickness. *Compos. Sci. Technol.* **2010**, *70*, 1660−1666.
(37) Matabola, K. P.; Vries, A. R.; Luyt, A. S.; Kumar, R. Studies on single polymer composites of poly(methyl methacrylate) reinforced with electrospun nanofibers with a focus on their dynamic mechanical properties. *Express. Polym. Lett.* **2011**, *5*, 635−642.
(38) Stachewicz, U.; Modaresifar, F.; Bailey, R. J.; Peijs, T.; Barber, A. H. Manufacture of void-free electrospun polymer nanofiber composites with optimized mechanical properties. *ACS Appl. Mater. Interfaces* **2012**, *4*, 2577−2582.
(39) Nao, H.; Takashi, T.; Hiroshi, U. Green composite of poly(3-hydroxybutyrate-co-3-hydroxyhexanoate) reinforced with porous cellulose. *ACS Sustainable Chem. Eng.* **2014**, *2*, 248−253.
(40) Uyama, H.; Kuwabara, M.; Tsujimoto, T.; Usuki, A.; Kobayashi, S. Green nanocomposites from renewable resources: Plant oil-clay hybrid materials. *Chem. Mater.* **2003**, *15*, 2492−2494.
(41) Nyambo, C.; Mohanty, A. K.; Misra, M. Polylactide-based renewable green composites from agricultural residues and their hybrids. *Biomacromolecules* **2010**, *11*, 1654−1660.
(42) Koronis, G.; Silva, A.; Fontul, M. Green composites: A review of adequate materials for automotive applications. *Composites, Part B* **2013**, *44*, 120−127.
(43) Lu, L. L.; Wu, D. F.; Zhang, M.; Zhou, W. D. Fabrication of polylactide/poly(ε-caprolactone) blend fibers by electrospinning: Morphology and orientation. *Ind. Eng. Chem. Res.* **2012**, *51*, 3682−3691.
(44) Rachele, P.; Loredana, T.; Vincenzo, V.; Vittoria, V. New nanohybrids of poly(ε-caprolactone) and a modified Mg/Al hydrotalcite: mechanical and thermal properties. *J. Polym. Sci., Part B: Polym. Phys.* **2007**, *45*, 945−954.
(45) Fowkes, F. M. Determination of interfacial tensions, contact angles and dispersion forces in surfaces by assuming additivity of intermolecular interactions in surfaces. *J. Phys. Chem.* **1962**, *66*, 382−382.
(46) Owens, D. K.; Wendt, R. C. Estimation of surface free energy of polymers. *J. Appl. Polym. Sci.* **1969**, *13*, 1741−1747.
(47) Van Oss, C. J.; Good, R. J.; Chaudhury, M. K. Additive and nonadditive surface tension components and the interpretation of contact angles. *Langmuir* **1988**, *4*, 884−891.
(48) Dalai, E. N. Calculation of solid surface tensions. *Langmuir* **1987**, *3*, 1009−1015.
(49) Wu, S. H. *Polymer Interface and Adhesion*; Marcel Dekker, Inc: New York, 1982.
(50) Deitzel, J. M.; Kleinmeyer, J.; Harris, D.; Beck Tan, N. C. The effect of processing variables on the morphology of electrospun nanofibers and textiles. *Polymer* **2011**, *42*, 261−272.
(51) Wu, D. F.; Sun, Y. R.; Yang, T.; Shi, T. J.; Zhai, L. F.; Zhou, W. D.; Zhang, M.; Zhang, J. Electrospinning of poly(trimethylene terephthalate)/carbon nanotube composites. *Eur. Polym. J.* **2011**, *47*, 284−293.
(52) Fong, H.; Chun, I.; Reneker, D. H. Beaded nanofibers formed during electrospinning. *Polymer* **1999**, *40*, 4585−4592.
(53) Wang, J. H.; Wu, D. F.; Zhang, M.; Zhou, W. D. Poly(vinylidene fluoride) reinforced by carbon fibers: Structural parameters of fibers and fiber-polymer adhesion. *Appl. Surf. Sci.* **2012**, *258*, 9570−9578.
(54) Ho, K. K. C.; Lamoriniere, S.; Kalinka, G.; Schulz, E.; Bismarck, A. Interfacial behavior between atmospheric-plasma-fluorinated carbon fibers and poly(vinylidene fluoride). *J. Colloid Interface Sci.* **2007**, *313*, 476−484.
(55) Han, D.; Steckl, A. J. Superhydrophobic and oleophobic fibers by coaxial electrospinning. *Langmuir* **2009**, *25*, 9454−9462.
(56) Jiang, L.; Zhao, Y.; Zhai, J. A lotus-leaf-like superhydrophobic surface: a porous microsphere/nanofiber composite film prepared by electrohydrodynamics. *Angew. Chem.* **2004**, *43*, 4338−4341.
(57) Lee, K.; Lyu, S.; Lee, S.; Kim, Y. S.; Hwang, W. Characteristics and self-cleaning effect of the transparent super-hydrophobic film having nanofibers array structures. *Appl. Surf. Sci.* **2010**, *256*, 6729−6735.
(58) Sas, I.; Gorga, R. E.; Joines, J. A.; Thoney, K. A. Literature review on superhydrophobic self-cleaning surfaces produced by electrospinning. *J. Polym. Sci., Part B: Polym. Phys.* **2012**, *50*, 824−845.
(59) Nuraje, N.; Khan, W. S.; Lei, Y.; Ceylan, M.; Asmatulu, R. Superhydrophobic electrospun nanofibers. *J. Mater. Chem. A* **2013**, *1*, 1929−1946.
(60) Wenzel, R. N. Surface roughness and contact angle. *J. Phys. Chem.* **1949**, *53* (9), 1466−1467.
(61) Cassie, A. B. D. Contact angles. *Discuss. Faraday Soc.* **1948**, *3*, 11−16.
(62) Lee, H. M.; Park, O. O. Rheology and dynamics of immiscible polymer blends. *J. Rheol.* **1994**, *38*, 1405−1425.
(63) Yu, W.; Bousmina, M.; Grmela, M.; Zhou, C. X. Modeling of oscillatory shear flow of emulsions under small and large deformation fields. *J. Rheol.* **2002**, *46*, 1401−1418.
(64) Dinh, S. M.; Armstrong, R. C. Rheological equation of state for semiconcentrated fiber suspensions. *J. Rheol.* **1984**, *28*, 207−227.
(65) Keshtkar, M.; Heuzey, M. C.; Carreau, P. J. Rheological behavior of fiber-filled model suspensions: Effect of fiber flexibility. *J. Rheol.* **2009**, *53*, 631−650.
(66) Wu, D. F.; Wu, L.; Zhang, M.; Zhao, Y. L. Viscoelasticity and thermal stability of polylactide composites with various functionalized carbon nanotubes. *Polym. Degrad. Stab.* **2008**, *93*, 1577−1584.